LMU LUDWIG-MAXIMILIANS-UNIVERSITÄT MÜNCHEN

Investigation of Finite Sources through Time Reversal

S41C-1859

S. Kremers[1], G. Brietzke[1], **H. Igel[1]**, C. Larmat[2], A. Fichtner[1], P. A. Johnson[2], L. Huang[2]

[1]LMU Munich, [2]Los Alamos Nat. Lab.

1 Introduction

Under certain conditions **time reversal** is a promising method to determine earthquake source characteristics without any a-priori information (except the earth model and the data). It consists of injecting flipped-in-time records (-> adjoint methods) from seismic stations within the model to create an approximate reverse movie of wave propagation (e.g., Larmat et al., 2007, 2008).

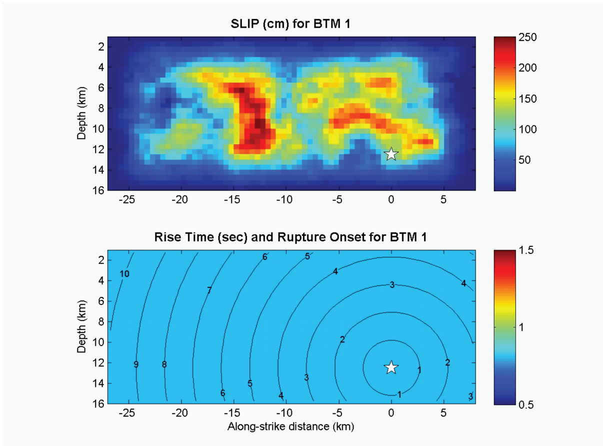

Fig 1. Slip distribution, hypocentre and rupture properties of our synthetic time reversal experiment.

We investigate the **potential of time reversal to recover finite source characteristics**. We use synthetic data from the **SPICE kinematic source inversion blind test** initiated to investigate the performance of current kinematic source inversion approaches (http://www.spice-rtn.org/library/valid). The synthetic data set attempts to reproduce the **2000 Tottori earthquake** with 33 records close to the fault. In this **progress report** we present initial simulations using a spectral-element code and discuss some of the observations.

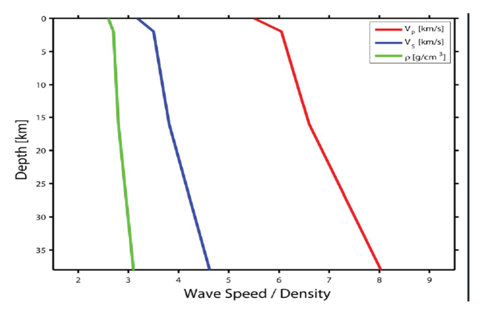

Fig 2. Velocity-depth model.

Key project questions:

- Which wavefield properties focus best (displacements, strains, rotations, energies?)
- Does the focusing clearly define the finite source rupture area?
- How does weighting of the adjoint sources affect the focusing properties?
- How well defined are source time, and hypocentre location?
- Is it possible to estimate rupture velocity? Can asperities be identified?
- What do we learn from this exercise for adjoint source inversion?
- Can we use time reversal in a more quantitative way to recover (finite) source properties?

2 SPICE Tottori benchmark

The SPICE kinematic source inversion blind test was initiated with the aim of investigating the performance of kinematic source inversion algorithms. The results (Mai et al., 2007) demonstrated the large uncertainties associated with source inversion. Here, we use the same data to investigate the **focusing properties of the time-reversed wavefield**.

All simulations presented here are carried out with a parallelized cartesian regular-grid spectral-element algorithm for the elastic wave propagation problem (e.g., Fichtner et al., 2009). The setup on a 120x120x32 (80x80x40 km) element grid with polynomial order 4 allows wavefield calculations up to 2Hz. To increase the frequency range the original velocity seismograms are injected as **accelerations**.

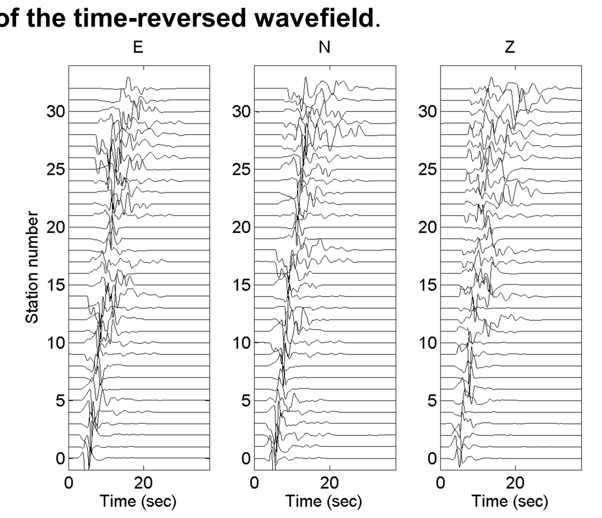

Fig 3. Synthetic velocity seismograms at 33 stations recorded for the finite fault given in Fig 1.

Time reversal and adjoint method

As is well known, injecting flipped-in-time (differential) seismograms at receiver position is one of the key ingredients of the adjoint method applied to the seismic inverse problem. In the case of structural inversion the adjoint sources consist of differential seismograms. For the problem of source inversion (assuming structure and hypocentre known) the adjoint approach leads to the re-injection of the whole seismogram. In the light of this, the time reversal can be considered a first step in an iterative source inversion process. The resulting reverse field (strains) leads to a source update (Tromp et al., 2005). Here we focus on the question whether **the rupturing fault area shows up in the time-reversed field in form of wave field focusing**.

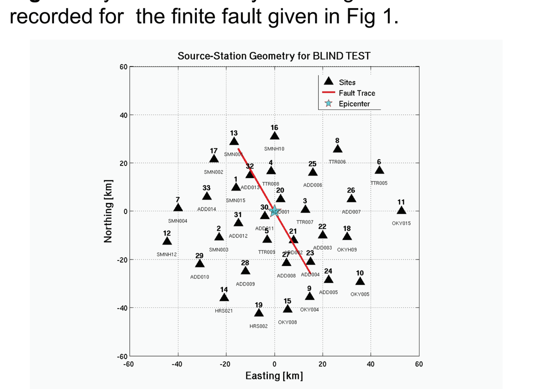

Fig 4. Station distribution above the fault (similar to the actual station distribution for the Tottori earthquake).

3 Time sequence at the surface and at depth

How does the **time-reversed wavefield** focus? This is not obvious as we inject low-frequency signals due to the large source extent, leading to long-wavelength features at depth. Injecting accelerations instead increases spatial frequencies.

In Fig. 5 snapshots (**x-component of acceleration**) are shown for time steps in which the rupture area (solid line) should be active. There are several issues/observations:

- The sources are injected right at the surface. Particularly the vertical components will generate **surface waves** that were not necessarily existent in the original wavefield. Thus, at the surface care needs to be taken with the interpretation of wavefront interference.
- While the station distribution is excellent in this synthetic study, several **stations are directly on the fault**. When reinjecting the seismograms, these stations are likely to dominate the entire wavefield in terms of amplitude (compare with Fig. 7).
- From a certain time the wavefield indeed concentrates in an area around the fault and **focuses as expected at the origin time and hypo(epi-)centre (bottom row)**.
- The rupture propagates in SE-NW direction. Some degree of focusing can also be observed in the opposite direction (SE), however with lower amplitude.
- The constructively interfering wavefield has high amplitude up to quite some distance away from the fault.

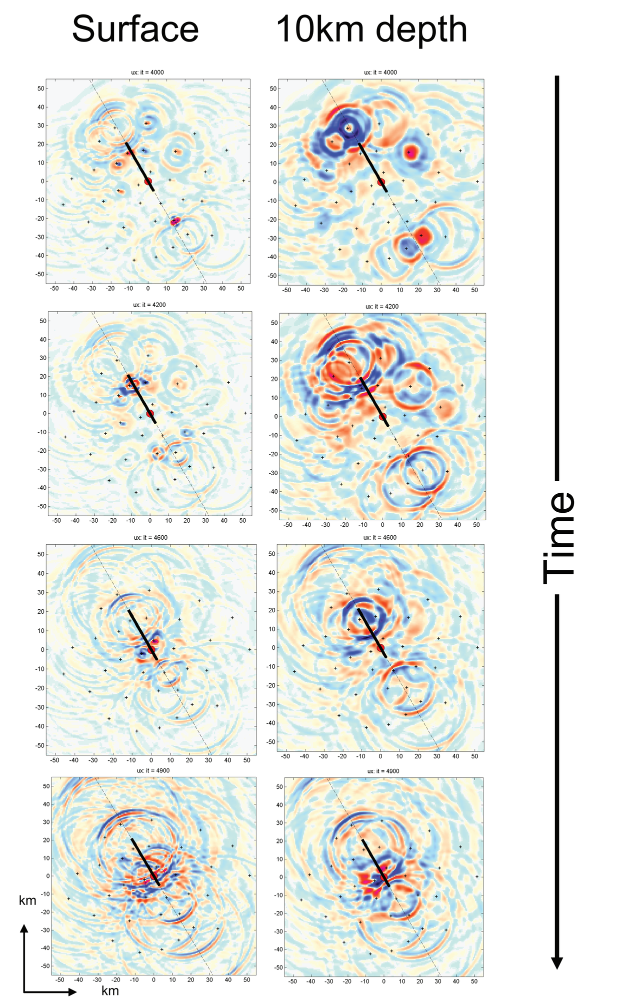

Fig 5. Snapshots of reverse field (x-component of acceleration). The fault strike is indicated by a broken line. The rupturing area is solid. Stations are indicated by ,+'. Left column: surface. Right column: 10km depth (compare with Fig. 1.). Bottom row corresponds approx. to origin time. Epicenter is indicated by a red dot.

4 Focusing properties of various fields

Which wavefield property focuses best? From an adjoint theory point of view the time-reversed **strain field** contains information on the source update.

In Fig. 7 we show snapshots of various fields at the time of expected focusing at the hypocenter. First, the polarities of (some of) the wavefields contain information on the source mechanism. The source mechanism in this example is a **pure strike-slip**.

Using the energy of the **rotational wavefield** (lower right corner) allows separating out the shear-wave field. The overall focusing in the fault region is most pronounced in the fields proportional to energy (summed squared translational or rotational components, bottom row, two right panels).

One of the remaining tasks is to find **objective criteria to constrain source volumes, fault orientations, source mechanisms, rupture speed** for a given station distribution.

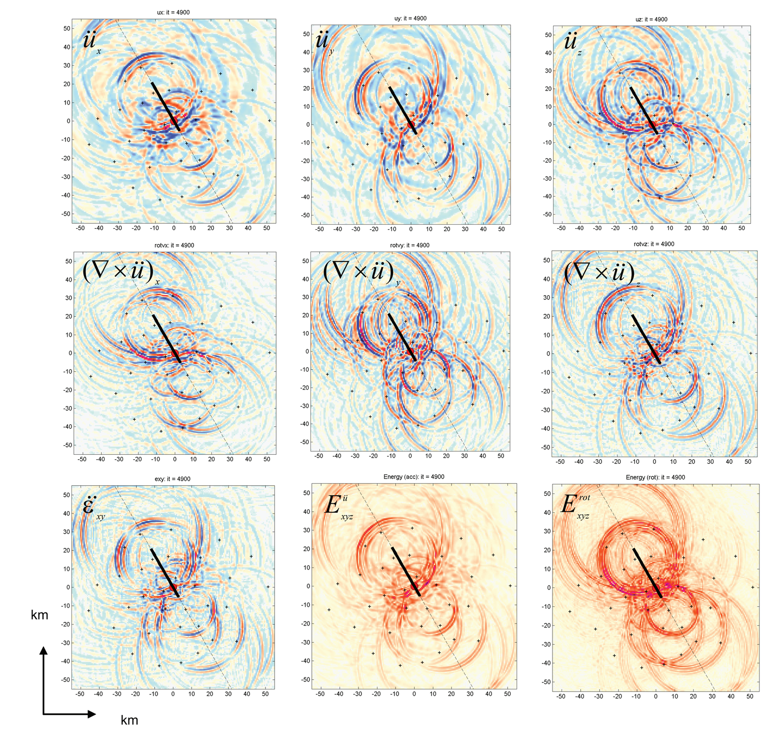

Fig 7. Snapshots (surface) at the expected time of focusing for various wavefield properties. Top row: x-, y-, and z-component of acceleration. Middle row: x-, y-, and z-component of the curl of the acceleration wavefield. Bottom row: xy-component of strain, sum of squared amplitudes (translations), sum of squared amplitudes (rotations).

5 Adjoint Source Weighting Cumulative Energy

Geometrical spreading will severely affect the time-reversed wavefield and focusing. Receivers at a distance from the fault will influence the focusing much less. This raises the question whether other weights are useful (e.g., taking into account distance from epicentre, fault distance, or uniform weighting).

In the right panel we compare results for a time-reversed wavefield (vertical component of rotation) with the **original seismograms** (the relative peak seismogram amplitudes are shown as circles, top left) and using **uniform weights** (top right). The snapshots at different times (original left, uniform weighting right) show that with uniform weighting more energy (and more constructive interference) is observed at the whole surface area (and at depth, not shown here).

We expect that the focusing of the wavefield from the various stations should appear when **the wavefield is integrated over time and space (here over seismogenic depth, 3-20km)**.

The results of integrated energies are shown in the bottom row (left, original weight; right, uniform weight). **We found the ruptured fault!** The original weighting clearly highlights the area of the rupture projected onto the surface (but compare with the figure top left). It is not surprising that we basically see the integrative energy focusing close to the receivers with largest amplitudes!

This effect is likely to mask the focusing from distant receivers.

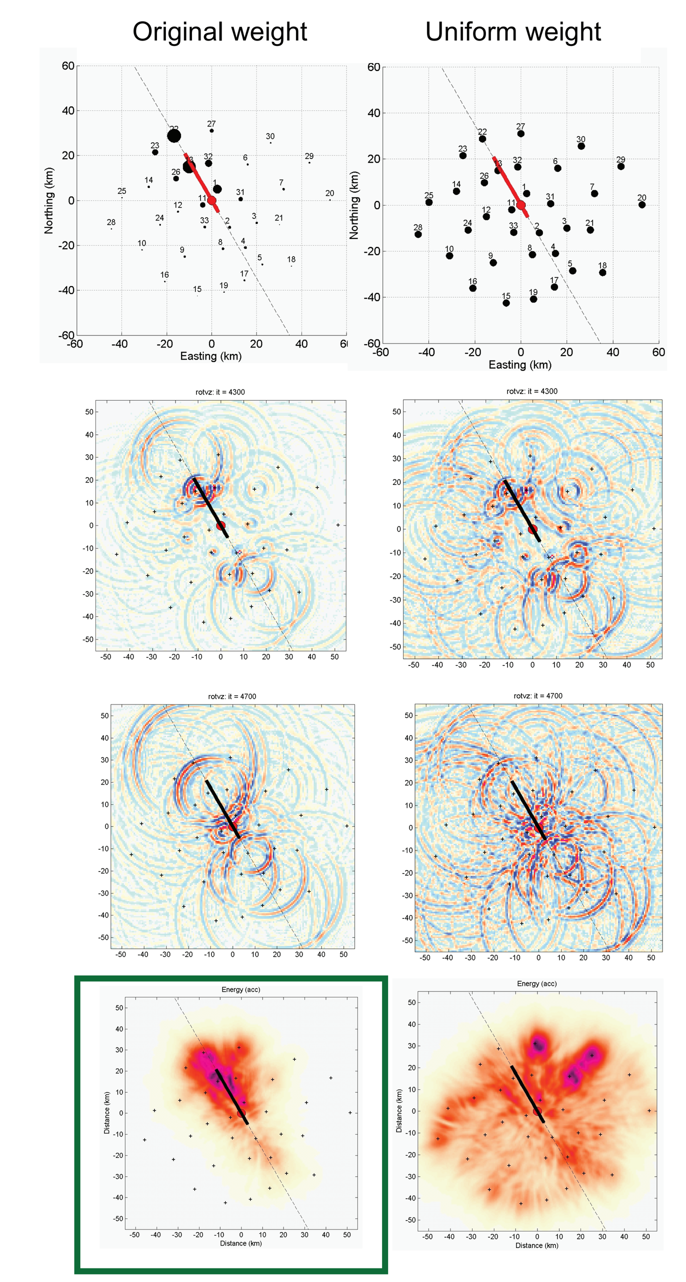

6 Projections on the fault

We relax the ignorance of the fault location and strike and investigate **the energy on the fault plane**. The snapshots on the right (left column) show the reversing wavefield (summed squared amplitudes) and the cumulative energy summed over depth (solid lines, bottom). Compare with the snapshots of energies summed over seismogenic depth (right column, horizontal plane).

We clearly see focusing at the hypocentre. **The cumulative energy integrated over time (bottom) highlights the ruptured fault area.**

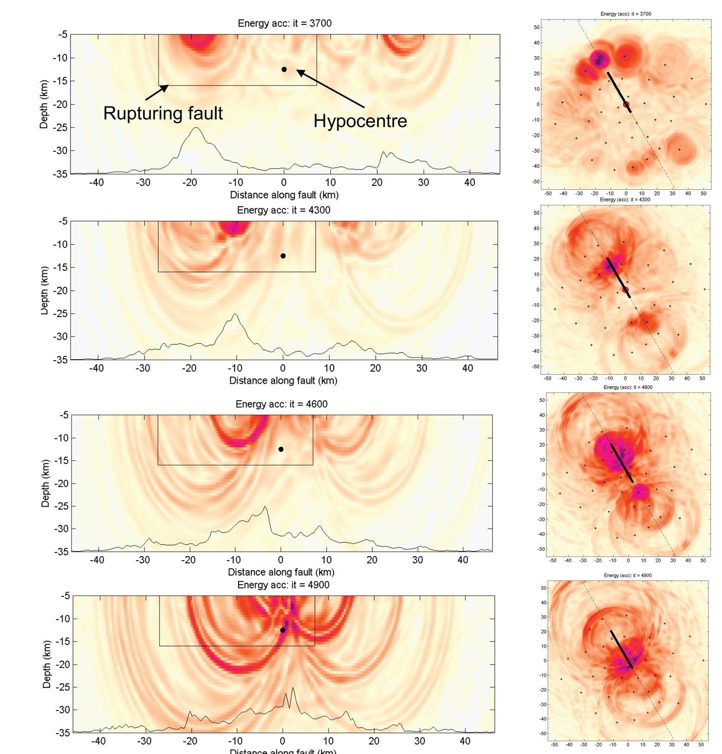

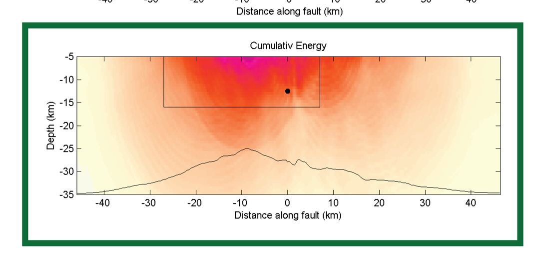

Cumulative energy on the fault integrated over time.

Conclusions

- **We time-reversed synthetic seismograms of the SPICE kinematic source inversion blind test.**
- **The cumulative energy of the reverse time field focuses at the hypocentre and the rupture area.**
- **Radiation by stations close to the fault dominates the wavefield. Uniform (or other) source weighting degrades the focusing on the rupturing area.**

References

Fichtner, A., Igel, H., Bunge, P., Kennett, B., (2009), Simulation and Inversion on continental scales based on the spectral element method, J. Numerical Analysis, Industrial and Applied Mathematics, submitted.

Mai M. et al., Earthquake Source Inversion Blindtest: Initial Results and Further Developments, AGU Fall Meeting 2007.

Larmat, C., J.-P. Montagner, M. Fink, Y. Capdeville, E. Clévédé, A. Tourin. (2007) Time-reversal Imaging of seismic sources and the Great Sumatra Earthquake. *Geophys. Res. Lett.,* 33, L19312.

Larmat, C., J. Tromp, Q. Liu, and J.-P. Montagner (2008), Time reversal location of glacial earthquakes, *J. Geophys. Res.*, 113, B09314.

Tromp, J., Tape, C., and Q. Liu, 2005, Seismic tomography, adjoint methods, time reversal, and banana-doughnut kernels, *Geophysical Journal International*, v. 160, p. 195-216

Acknowledgments

HI and SK acknowledge support by LANL for their visits to LANL in 2008. GB was supported by the KONWIHR project.